

# Supplemental Materials

## Supplemental methods

### Isolation of adipocytes from dWAT and other fat pads

Mice were anesthetized by ketamine/xylazine cocktail, shaved and the dorsal skin (NAIR treatment for only 40 seconds to avoid damage to skin) was chemically depilated, then the skin was washed by warm water and dried with gauze. Thereafter, the skin was allowed to dry for 2 more minutes. The depilated skin was cleaned with ethanol pads. The dorsal skin was cut carefully, and as much as possible removed as much as possible of the subcutaneous fat attached to the skin. The tissue was placed in a 50 ml conical tube with DMEM/F-12 medium (Gibco). Each tube contained dorsal skin from 3-4 mice. For other fat pads, fat from the same depots were pooled together, and also put into DMEM/F-12 medium. The skin or other fat pads were washed twice with warm DMEM/F-12 medium. For the skin, it was cut into big pieces, removed the extra tissues associated with the skin, and we floated the skin on the DMEM/F-12 medium with 1.8U/ml Dispase (Invitrogen), 1U/ml Collagenase D (Roche). We incubated the floating skin in a 37°C cell incubator for 90min-120min. We carefully took the skin out of the digestion medium, and put it into a 6cm dish with 37°C DMEM/F-12 DMEM/F-12 medium. We gently dissociated the dWAT layer into the medium, and tried not to disturb the dermis. We subsequently filtered the dissociated cells with a 100  $\mu$ m cell strainer into a new 50 ml conical tube, centrifuged at 600g for 5min. Dermal adipocytes floated on top of the medium after centrifugation and could be seen as a white layer. We transferred the mature adipocytes to a tube with 37°C DMEM/F-12 DMEM/F-12 medium with a Pasteur pipette, gently mixed it and centrifuged at 600g for 5 min. We then

transferred the floating dermal adipocytes to a 1.5ml tubes with 1 ml 37°C DMEM/F-12 DMEM/F-12 medium with a Pasteur pipette, centrifuged at 600g for 2 min, and removed the medium with a syringe with long needle. We then snap froze the dermal adipocytes for later usage. For isolation of adipocytes from other fat pads, we cut the fat to very small pieces, and incubated it in DMEM/F-12 medium with 1 U/ml Dispase, 1U/ml Collagenase D for 1 hour while shaking the tubes gently every 10 min during the digestion. Gently pipetted the fat tissues by Pasteur pipette, and filtered the dissociated cells with 100  $\mu$ m cell strainer to a new 50 ml conical tube, centrifuged at 600g for 5min. Adipocytes floated on top of the medium after centrifuge and represented as a white layer. Transferred the mature adipocytes to a tube with 37°C DMEM/F-12 DMEM/F-12 medium by Pasteur pipette, gently mixed it and centrifuged at 600g for 5 min. Transferred the floating adipocytes to a 1.5ml tubes with 1 ml 37°C DMEM/F-12 DMEM/F-12 medium by Pasteur pipette, centrifuged at 600g for 2 min, and got rid of the medium by a syringe with long needle. Snap froze the adipocytes for later usage. If the cells were used for metabolite analysis, the cells were washed a with large volume of warm PBS once quickly, then snap froze the sample.

### **NMR fat mass analysis**

Fat mass of was measured using a Bruker Minispec mq10 (Bruker).

### **Isolation of single cell suspension from skin**

Mice were anesthetized by ketamine/xylazine cocktail, shaved and chemically depilated the dorsal skin (NAIR only 40 seconds to avoid damage of skin), then washed the skin with warm water and dried the skin with gauze. Thereafter, we let the skin dry for 2 more minutes. We cleaned the depilated skin with ethanol pads. Using a 10 mm punch

or scissors, the desired piece of skin cleared of subcutaneous fat attached to the skin, and the skin was placed in a 50 ml conical tube with 4°C DMEM/F-12 medium (Gibco) until ready to process. The skin was transferred directly into a petri dish, placed in the lid of the petri dish without medium and then minced it to small pieces, then transferred into a 15ml tube with 5 ml fresh digestion buffer (RPMI 1640 medium with 1.7U/ml Liberase TL (Roche, 05401020001), 100 U/ml Penicillin-Streptomycin (Gibco, 15140), 0.01% DNase (Sigma, DN25), and 0.05 mM  $\beta$ -mercaptoethanol (Thermofisher)). The tube was placed laying down on a shaker at 100rpm at 37 °C for 1-2 hours. Digestion time depended on the age and gender. Young mice and female mice required less time for full digestion. The digested skin was gently pipetted, each sample was filtered over a 50 ml conical tube using a 40  $\mu$ m cell strainer. Using the rubber of a syringe to mash the tissue left in the strainer, washed the strainer with 20 ml RPMI 1640 medium, and more medium was added to the tube until the medium was not viscous anymore. Cells were spun down at 600g for 10 min. Red blood cells were removed with ACK buffer (Invitrogen). The cells were re-suspended, filtered through a 40  $\mu$ m cell strainer again, and spun at 300g for 5 min. Cells were re-suspended in medium for culture or for other usage.

### **Cell culture and differentiation**

AdipoChaser-mTmG mice were fed with Dox chow diet (P28-P35), then switched to normal chow diet, skins were harvested around P56-P63. Single cell suspensions were obtained from skin as described above. FACS sorted CD31<sup>-</sup>/CD45<sup>-</sup>/PDGFR $\alpha$ <sup>+</sup>/GFP<sup>-</sup> and CD31<sup>-</sup>/CD45<sup>-</sup>/PDGFR $\alpha$ <sup>+</sup>/GFP<sup>+</sup> cells were plated in 48-well plates in growth media

containing DMEM/F12 (Invitrogen) and 10% fetal bovine serum (FBS). For spontaneous differentiation, cells were cultured in medium containing 2%FBS and ITS supplement [60% pH7–7.4 low glucose DMEM, 40% pH 7.25 MCDB201 (Sigma M6770), 1% ITS premix (Insulin-Transferrin-Selenium) (BD Bioscience 354352), 0.1 mM L-ascorbic acid-2-phosphate (Sigma A8960-5G), 10 ng/mL FGF basic (R&D Systems, 3139-FB-025/CF), Pen/Strep, and gentamicin and incubated at 37°C in 10% CO<sub>2</sub>. Media was replaced every other day and spontaneous adipogenesis were evaluated after 14 days of culture. For TGFβ-induced myofibroblast differentiation, cells were treated with human recombinant TGFβ (1ng/mL) for 8 days and cells were harvested for gene expression analysis of fibrotic markers.

### **Immunofluorescence**

The following antibodies and concentrations were used: chicken anti-GFP 1:700 (Abcam ab13970); guinea pig anti-perilipin 1:1500 (Fitzgerald 20R-PP004); mouse anti-Alpha-Smooth Muscle Actin Monoclonal Antibody (1A4), eBioscience™ (Thermo Fisher, 14-9760-80), BrdU (BD Biosciences, 550891) rabbit anti-phospho-HSL<sup>S660</sup> (CST, 4126), goat anti-guinea pig Alexa 647 1:200 (Invitrogen, A21450), goat anti-guinea pig Alexa 488 1:200 (Invitrogen, A11073), goat anti-chicken Alexa 488 1:200 (Invitrogen, A11039), goat anti-mouse Alexa 647 1:200 (Invitrogen, A28181), goat anti-rabbit Alexa 647 1:200 (Invitrogen, 27040). Briefly, paraffin sections were dewaxed and hydrated in Xylene and Ethanol and ddH<sub>2</sub>O. Slides were placed in chambers containing 1% R-Buffer Buffer A pH 6.0 solution and antigen retrieval was done using Antigen Retriever 2100 (Electron Microscopy Sciences) for 2 hours. Following PBS wash for 5 minutes, FX Signal Enhancer (Invitrogen, I36933) was added to the slides for 30 minutes at room

temperature. Slides were then blocked for 30 minutes in PBS containing 10% normal goat serum (Invitrogen, 01-6201) at room temperature. Primary antibodies were then diluted in PBS containing 10% normal goat serum and added to paraffin sections overnight at 4°C. Following washes in PBS, slides were then incubated with secondary antibodies diluted in PBS containing 10% normal goat serum for 2 hours at room temperature. Washed slides were then mounted with Prolong Anti-Fade mounting medium containing DAPI (Invitrogen, P36941). All Images were obtained using Keyence BZ-X710 microscope or Zeiss LSM 880 confocal microscope (Live cell Imaging Facility, UT Southwestern Medical Center).

### **RNA-seq**

Total RNA was extracted by RNeasy Mini Kit (Qiagen). Samples were run on the Agilent 2100 Bioanalyzer to determine level of degradation thus ensuring only high quality RNA is used (RIN Score 8 or higher). The Qubit fluorometer was used to determine the concentration prior to starting library preparation. 1 µg of total DNase treated RNA was then prepared with the TruSeq Stranded Total RNA LT Sample Prep Kit from Illumina. Total RNA was depleted of its rRNA and fragmented before strand specific cDNA synthesis. cDNA was then a-tailed and indexed adapters were ligated. After adapter ligation, samples were PCR amplified and purified with Ampure XP beads, then validated again on the Agilent 2100 Bioanalyzer. Samples were quantified by Qubit before being normalized and pooled, then run on the Illumina HiSeq 2500 using SBS v3 reagents. The whole process was performed at the UTSW Next Generation Sequencing (NGS) Core at McDermott Center with the standardized protocol.

### **Quantitative RT-qPCR**

RNA from freshly sorted cells or cultured cells was extracted by RNeasy Mini Kit (Qiagen) or Trizol (Invitrogen) according to manufacturer's instructions. cDNA was synthesized by using the iScript™ cDNA Synthesis Kit (Biorad, 170-8891). Gene expression differences were determined by quantitative PCR using SYBR Green PCR Master Mix (Applied Biosystems). Values were normalized to reference genes using the  $\Delta\Delta$ -Ct method. Unpaired Student's t-test was used to evaluate statistical significance. All primer sequences are listed within the primer table.

### **Flow cytometry**

Cells from the skin suspension were first incubated on ice for 10 minutes in 400  $\mu$ L FACS buffer (DPBS with 2% FBS, 0.1 mM EDTA) containing anti-mouse CD16/CD32 Fc Block (clone 2.4G2) (BD, 553141, 1:200). Cells were then incubated with primary antibody (anti- PerCP/Cy5.5 anti-mouse CD31 antibody 1:400 (Biolegend, 102419), PerCP/Cy5.5 anti-CD45 antibody 1:400 (Biolegend, 103131), APC anti-mouse CD140a antibody (PDGFR $\alpha$ ) 1:200 (Biolegend, 135907)), and were incubated rotating at 4°C for 20 minutes. They were then washed three times with FACS buffer, and either analyzed using a FACSCantoII™ flow cytometer or sorted by a FACS Aria™ flow cytometer (UT Southwestern Medical Center Flow Cytometry Core Facility). For sorting, cells were initially selected by size, on the basis of forward scatter (FSC) and side scatter (SSC). Live cells were then gated on both SSC and FSC- Width singlets, ensuring that individual cells were analyzed. Cells from wild-type mice, non-dox-fed mice, along with single stained controls were used to determine background fluorescence levels and for compensation. Cells were sorted into FBS and then either cultured or prepared for RNA extraction.

## **Metabolite analysis**

Snap frozen adipocytes (50 mg) were homogenized with a mechanical tissue disruptor in 0.8 ml of 80% methanol in a screw cap borosilicate glass tube. The homogenizer probe was rinsed with 0.8 ml of 80% MeOH and the methanolic solution was combined with the homogenate. The tissues were kept on ice during the homogenization/quenching process. Immediately afterwards 20  $\mu$ l of Internal solution was added (7-methyluric acid ( $2,4,5,6$ - $^{13}\text{C}_4$ , 99%,  $1,3,9$ - $^{15}\text{N}_3$ , 98%) 25  $\mu\text{g/ml}$ . (Cambridge Isotope Laboratories, Inc., Tewksbury, MA). Samples were thoroughly vortexed and then centrifuged in a benchtop centrifuge at 2,500 g (Sorvall Legend XTR, Thermo Fisher Scientific, Waltham, MA). Supernatant was transferred to a 5.0 ml polypropylene cell culture tube. Protein pellets were re-extracted with 1 mL of 80% MeOH and the supernatants were combined. Tissue extracts were dried in a speed-vap concentrator. The dried residues were reconstituted in 220  $\mu$ l of  $\text{H}_2\text{O}$  0.1% Formic Acid and transferred to GC vials. In the case of adipose tissue samples, a second set of samples was prepared at a 1:50 dilution from the original reconstituted sample. TCA intermediates were analyzed by injecting 1  $\mu$ l of sample to the LC/MS/MS system consisting of a Shimadzu LCMS-8060 triple quadrupole mass spectrometer operating the DUIS ion source in electrospray mode (Shimadzu Scientific Instruments, Columbia, MD) coupled to a Nexera X2 UHPLC chromatographer equipped with three pumps, autos-amplifier SIL-30AC and CTO-20AC (Shimadzu Scientific Instruments). Compounds were resolved and analyzed using the instrumental parameters and chromatographic conditions described in the Shimadzu LC/MS/MS method package for cell culture profiling (Shimadzu Scientific Instruments).

## Supplemental Figure Legends:

### Figure S1. Screening of marker gene expression for dermal adipocytes.

(A) dWAT layer peeled from skin after 30min-1h digestion (left). Dermal adipocytes dissociated from skin after 90-120min digestion. (B) Hierarchical clustering of transcriptional profiles from dermal and inguinal adipocytes. Labels identify genes showing enrichment gene ontology analyses (n=2 samples, each sample contained adipocytes from 4 mice), FC: fold change. (C-D) Gene ontology analysis of the RNA-seq results. Pathways upregulated (C) and downregulated (D) more than two-fold in dermal adipocytes. (E) Expression profile of *Ccl4* in different adipocytes, fat pads, and tissues in 2-month-old mice (n=2). Similar results obtained in 3 independent experiments. (F) *Ccl4* gene expression in 30-day-old mice. (n=6-7, each sample pooled from 3-4 mice). Similar results obtained in 3 independent experiments. Data are shown as mean  $\pm$  SD. *P* values were calculated with two-tailed student's t test. A *P* value less than 0.05 is considered significant. \**P*<0.05, \*\**P*<0.01.

### Figure S2. dWAT showed dynamic changes with different stimuli.

(A) The oscillation of dWAT with hair cycling. n=3/group. Scale bars: 200 $\mu$ m. (B) Quantification of dWAT thickness in (A). (C) High fat diet efficiently stimulated the expansion of dWAT in a time dependent manner. n=3/group. Scale bars: 200 $\mu$ m. (D) Quantification of dWAT thickness in (C). (E) No obvious multilocular cells were observed in dWAT layer after cold exposure to 6°C. n=3/group. Scale bars: 200 $\mu$ m. (F) Quantification of dWAT thickness in (E). (G) H&E staining of subcutaneous fat of vehicle/CL316243 treatment mice. Scale bars: 100 $\mu$ m. (H) Comparative histology of skins of vehicle and bleomycin treated mice. Dermal adipocytes disappeared after 3 weeks of bleomycin treatment. n=3/group. Scale bars: 200 $\mu$ m. (I) Quantification of dWAT thickness in (H). (J) H&E staining of skin at indicated time points (left, Scale bars: 200 $\mu$ m.),

pHSL<sup>S660</sup> (red) was detected in dermal adipocytes during the regression of dWAT layer (right, Scale bars: 100 $\mu$ m.). Adipocytes were stained with Perilipin1 (PLIN1) (green). Nuclei were stained with DAPI (blue). n=2/group. **(K)** Quantification of dWAT thickness in **(J)**. **(L)** 28-day-old mice were fed with Niacin water for 1 and 3 weeks separately to inhibit lipolysis. Dermal adipocytes were stained by PLIN1. Niacin treated mice showed larger adipocytes that regressed more slowly than those of control group. n=5/group. Scale bars: 200 $\mu$ m. **(M)** Quantification of the size of dermal adipocytes in **(L)**. **(N)** 28-day-old mice were topically applied with vehicle or Atglistatin, an inhibitor for lipolysis, twice daily for a total of 5 days. Atglistatin treated group showed impaired lipolysis as indicated by the larger dermal adipocytes. n=5/group. Scale bars: 200 $\mu$ m. **(O, P)** Quantification of dWAT thickness and the size of dermal adipocytes in **(N)**. Results were confirmed in three independent experiments. Data are shown as mean  $\pm$  SD. *P* values were calculated with two-tailed student's *t* test (**I, O, P**), or two-way ANOVA with Tukey's test (**B, D, F, K, M**). A *P* value less than 0.05 is considered significant. \**P*<0.05, \*\**P*<0.01. 2X magnification for insets.

**Figure S3. De novo adipogenesis contributed to the expansion of dWAT during developmental stage, while re-appearing of pre-existing adipocytes contributed more to the expansion of dWAT in adult mice.**

**(A)** Schematic overview of the AdipoChaser-mTmG model. **(B)** Experiment design: labeling the pre-existing adipocytes generated from the first anagen, and traced to P30 and adult. **(C)** Pregnant mice were put on Dox (E18.5-P17), skin was harvested at P17 from the offspring (pulse). Thereafter, mice were fed with chow diet, and harvested skin at P30 (P30). Mice were fed with HFD (P63-P77) to induce the expansion of dWAT layer and harvested skin at P77 (HFD). Hair was depilated at P63, and skin harvested at P74-P77 (Depilation). n=5/group. **(D)** Quantification of the number originally labeled adipocytes and new generated adipocytes in **(C)**.

(E) Experiment design: labeling the pre-existing adipocytes at the second anagen, and traced following twice depilation. (F) Mice were put on Dox (P28-P35). Then mice were switched to chow diet, and depilated the hair at P63. Depilated hair again at P100, harvested skin around P112 (Twice depilation). n=5/group. (G) Quantification of the number originally labeled adipocytes and new generated adipocytes in (F). (H) Experimental design: labeling the pre-existing adipocytes at the second anagen and traced the adipocytes for 6 months. (I) After 7 days of Dox chow diet (P28-P35), skins were harvested at P35 (pulse). Thereafter, mice were fed with chow diet, and harvest skin at 7 months old. (J) Quantification of the number originally labeled adipocytes and newly generated adipocytes in (I). PLIN1 only cells were marked with yellow asterisk. n = 3-4/group. Results were confirmed in three independent experiments. Data are shown as mean  $\pm$  SD. *P* values were calculated with two-tailed student's *t* test (G, J) or one-way ANOVA with Dunnett test (D). A *P* value less than 0.05 is considered significant. \**P*<0.05, \*\**P*<0.01. Scale bars: 100 $\mu$ m.

**Figure S4. Single cell RNA-seq reveals two distinct fibroblast subpopulations.**

(A) GFP<sup>+</sup>PLIN1<sup>-</sup> fibroblast-like cells were detected in skin of Dox treatment AdipoChaser-mTmG mice. Scale bars: 100 $\mu$ m. n=3 mice. (B) Clustering of transcriptomes of CD31<sup>-</sup>/CD45<sup>-</sup>/PDGFR $\alpha$ <sup>+</sup>/GFP<sup>+</sup> fibroblasts isolated from two-month-old mice (Dox: P28-P35). Each cell is represented as a dot, assigned to a cluster by a clustering algorithm, and plotted on the t-SNE graph. The plot reveals two distinct clusters, termed cluster 1 (Blue) and cluster 2 (Orange) (C-D) GO analysis of genes upregulated (C) or downregulated (D) in Cluster 1 compared to that of Cluster 2 in CD31<sup>-</sup>/CD45<sup>-</sup>/PDGFR $\alpha$ <sup>+</sup>/GFP<sup>+</sup> fibroblasts. (E) Heat map of top 25 most differentially expressed genes between cluster 1 and cluster 2 in CD31<sup>-</sup>/CD45<sup>-</sup>/PDGFR $\alpha$ <sup>+</sup>/GFP<sup>+</sup> fibroblasts. (F) Clustering of transcriptomes of CD31<sup>-</sup>/CD45<sup>-</sup>/PDGFR $\alpha$ <sup>+</sup>/GFP<sup>-</sup> fibroblasts isolated from two-

month-old mice (Dox: P28-P35). **(G-H)** GO analysis of genes upregulated (G) or downregulated (H) in Cluster 1 compared to that of Cluster 2 in CD31<sup>-</sup>/CD45<sup>-</sup>/PDGFR $\alpha$ <sup>+</sup>/GFP<sup>-</sup> fibroblasts. **(I)** Heat map of top 25 most differentially expressed genes between cluster 1 and cluster 2 in CD31<sup>-</sup>/CD45<sup>-</sup>/PDGFR $\alpha$ <sup>+</sup>/GFP<sup>-</sup> fibroblasts. **(J)** Unbiased clustering of combined CD31<sup>-</sup>/CD45<sup>-</sup>/PDGFR $\alpha$ <sup>+</sup>/GFP<sup>-</sup> and CD31<sup>-</sup>/CD45<sup>-</sup>/PDGFR $\alpha$ <sup>+</sup>/GFP<sup>+</sup> cells on the t-SNE graph. **(K)** The number and ratio of GFP<sup>-</sup> and GFP<sup>+</sup> cells in each cluster. **(L)** Distribution of GFP<sup>-</sup> and GFP<sup>+</sup> cells in clusters plotted on the t-SNE graph. **(M)** Cell cycle distribution in clusters plotted on the t-SNE graph. Scale bars: 100  $\mu$ m. 3X magnification for insets.

**Figure S5. *In vitro* culture and stimulation of de-differentiated dermal adipocytes.**

Mice were put on normal chow/Dox diet during second anagen (Dox: P28-P35), then they were switched to normal chow diet until a prolonged period in the second telogen. Skin was collected around P56-P60. **(A)** skin was digested, all the cells obtained from the skin were seeded in plate. GFP<sup>+</sup> cells were only detected in skin from *Adiponectin*<sup>rtta</sup> *TRE-Cre Rosa26*<sup>mTmG</sup> Dox<sup>+</sup> mice, but not that in *Adiponectin*<sup>rtta</sup> *Rosa26*<sup>mTmG</sup> Dox<sup>+</sup>, *Adiponectin*<sup>rtta</sup> *TRE-Cre Rosa26*<sup>mTmG</sup> Dox<sup>-</sup> mice (n=3/group). **(B)** Isolation of CD31<sup>-</sup>/CD45<sup>-</sup>/PDGFR $\alpha$ <sup>+</sup>/GFP<sup>-</sup> and CD31<sup>-</sup>/CD45<sup>-</sup>/PDGFR $\alpha$ <sup>+</sup>/GFP<sup>+</sup> cells from skin of *Adiponectin*<sup>rtta</sup> *TRE-Cre Rosa26*<sup>mTmG</sup> Dox<sup>+</sup> mice by FACS. The isolated cells were cultured in ITS medium for spontaneous differentiation. CD31<sup>-</sup>/CD45<sup>-</sup>/PDGFR $\alpha$ <sup>+</sup>/GFP<sup>+</sup> cells showed higher ratio of differentiation than that of CD31<sup>-</sup>/CD45<sup>-</sup>/PDGFR $\alpha$ <sup>+</sup>/GFP<sup>-</sup> cells (n=3 mice). **(C)** RT-PCR analysis of adipocyte marker gene expression in differentiated CD31<sup>-</sup>/CD45<sup>-</sup>/PDGFR $\alpha$ <sup>+</sup>/GFP<sup>-</sup> and CD31<sup>-</sup>/CD45<sup>-</sup>/PDGFR $\alpha$ <sup>+</sup>/GFP<sup>+</sup> cells (n=3 mice). **(D)** Isolation of CD31<sup>-</sup>/CD45<sup>-</sup>/PDGFR $\alpha$ <sup>+</sup>/GFP<sup>-</sup> and CD31<sup>-</sup>/CD45<sup>-</sup>/PDGFR $\alpha$ <sup>+</sup>/GFP<sup>+</sup> cells from skin of *Adiponectin*<sup>rtta</sup> *TRE-Cre Rosa26*<sup>mTmG</sup> Dox<sup>+</sup> mice by FACS. The isolated cells were stimulated with vehicle/TGF- $\beta$ . Fibrosis related genes were measured by RT-PCR (n=3 mice). Results were confirmed in three independent experiments. Data are shown as mean  $\pm$  SD. *P* values were calculated with

two-tailed student's t test (C) or two-way ANOVA with Tukey's test (D). A *P* value less than 0.05 is considered significant. \**P*<0.05, \*\**P*<0.01. Scale bars: 100 $\mu$ m.

**Figure S6. *Pparg*<sup>AKO</sup> mice show delayed hair coating and development.**

(A) Photographs of *Pparg*<sup>fl/fl</sup> and their littermate *Pparg*<sup>AKO</sup> mice at P6.5 and P14. *Pparg*<sup>AKO</sup> mice show growth retardation and delayed hair coat. (B) *Pparg*<sup>AKO</sup> mice developed fatty liver at very young age. (C) H&E staining showed that *Pparg*<sup>AKO</sup> mice have less dWAT volume, and display delayed hair cycling (n=5/group). (D-F) Quantification of dWAT thickness and hair cycle stage of hair follicles in *Pparg*<sup>fl/fl</sup> and *Pparg*<sup>AKO</sup> mice with different age. Results were confirmed in three independent experiments. Data are shown as mean  $\pm$  SD. *P* values were calculated with two-way ANOVA with Dunnett test. A *P* value less than 0.05 is considered significant. \**P*<0.05, \*\**P*<0.01. Scale bars: 200 $\mu$ m.

**Figure S7. Manipulation of dWAT reveals the roles of dermal adipocytes in maintaining skin morphology and function.**

(A) 7-day-old FAT-ATTAC and their littermate mice were injected with dimerizer (one injection every 3 days, injected until P33), skins were collected at the indicated time points for H&E staining. No negative impact on hair cycling is observed. The depletion of dermal adipocytes increased the thickness of the dermis in FAT-ATTAC mice during hair cycling (n=5/group). Scale bars: 200 $\mu$ m. (B) Quantification of the dWAT thickness in (A). (C-E) Dams were fed with Chow or HFD when their offspring was 7 days old. The body weight of the offspring was measured (n=8 mice/group) (C). The skin was collected at the indicated time points for H&E staining (D). Scale bars: 200 $\mu$ m. No negative impact on hair cycling was observed. Quantification of the dWAT thickness in mice with Chow/HFD from 7 days old (E). (F) The HFD fed mice showed different levels of hair loss around weaning age (P20-P28). (G) H&E staining

showed that hair shafts were broken in the hair follicle. Scale bars: 50 $\mu$ m. (H) 2-month-old FAT-ATTAC mice were injected with dimerizer to ablate adipocytes (one injection in every 3 days) or were injected with vehicle. Photographs of splinted excisional wounds on the dorsal skin of WT and FAT-ATTAC mice, revealing that FAT-ATTAC mice showed delayed wound healing (n=5/group). (I) H&E staining revealed that FAT-ATTAC mice showed delayed wound healing, as well as a thinner wound bed than what was observed for WT controls (n=5/group). Scale bars: 500 $\mu$ m. (J) *ADIPOQ* expression in active keloid lesion and adjacent control normal skin tissue from human (GSE90051) Two-condition experiment, active keloid lesion vs. adjacent control normal skin tissue. Paired sample from 7 individuals. (K, L) *ADIPOQ* and *CAMP* expression in human skin biopsies before and after wound (GSE124161), n=3 individuals for each time point. Results were confirmed in three independent experiments. Data are shown as mean  $\pm$  SD. *P* values were calculated with two-way ANOVA with Dunnett test. A *P* value less than 0.05 is considered significant. \**P*<0.05, \*\**P*<0.01.

**Table S1. PCR Primer table.**

qPCR primer sequences used in this study

Gene	Forward 5'-3'	Reverse 5'-3'
<i>Zfp423</i>	CAGGCCCAAGAAGAACAAG	GTATCCTCGCAGTAGTCGCACA
<i>Pparg2</i>	ATGTCTCACAATGCCATCAGGT	CAAATGCTTTGCCAGGGCTC
<i>Adiponectin</i>	CTGCAACATTCCGGGACTCTA	TCGTAGGTGAAGAGAACGGC
<i>Fabp4</i>	GGGATGGAAAGTCGACCACA	TCTTGTGGAAGTCACGCCTTT
<i>Ucp1</i>	GTGTGGCAGTGTTCAATGGG	GCATTGTAGGTCCCCGTGTA
<i>Cidea</i>	GGCCGTGTTAAGGAATCTGC	GCTCTTCTGTATCGCCCAGT
<i>Prdm16</i>	GCGTCCATCGCGAGAAATA	GGGAGTGGGGAAAGTTAGGC
<i>Adipsin</i>	CTACATGGCTTCCGTGCAAGT	AGTCGTCATCCGTCCTCCAT
<i>Col1a1</i>	GACCCTAACCAAGGCTGCAA	AGACGGCTGAGTAGGGAAC
<i>Col3a1</i>	ATTCTGCCACCCCGAACTCAA	ACAGTCATGGGGCTGGCATTT
<i>Acta2</i>	GATCACCATTGGAAACGAACGC	AGCATAGAGATCCTTCTGATGTC
<i>Fn1</i>	GAGAGCACACCCGTTTTTCATC	GGGTCCACATGATGGTGACTT
<i>Timp1</i>	CTTGGTCCCTGGCGTACTC	ACCTGATCCGTCCACAAACAG
<i>Tgfb1</i>	TTTAGGAAGGACCTGGGTTGG	TGTTGGTTGTAGAGGGCAAGG
<i>Camp</i>	AGCTACCTGAGCAATGTGCC	TTCTTGAACCGAAAGGGCTGT
<i>Ccl4</i>	CCAGGGTCTCAGCACCAAT	TTGGAGCAAAGACTGCTGGT
<i>Leptin</i>	GCGGTTGGATGGACTAGGAT	TTCGTCAGGGGCTTCCAAAG
<i>WT1</i>	GAGAGCCAGCCTACCATCC	GGGTCCTCGTGTTTGAAGGAA
<i>Serpinh1</i>	AGCTAAGTTCCAAGGCGACC	GGCTTTACCACCCAGTGACA
<i>Vim</i>	TGCTTCAAGACTCGGTGGAC	AAGCGCACCTTGTGCGATGTA
<i>Fsp</i>	TGCACCCAAACCGAAGTCATA	TTGGGGACACCTTTTAGCATCT
<i>P4hb</i>	TGGTGGACTCAAGCGAAGTG	ACACCACTGTTGGACGTGAT
<i>Fasn</i>	AGCTACCGGGCAAAGATGAC	GTGATAAGGTCCACGGAGGC
<i>Lpl</i>	GTGGACATCGGAGAACTGCT	CCTCTCGATGACGAAGCTGG
<i>Cebpa</i>	GCCGCTGGTGATCAAACAAG	AGTGCGCGATCTGGAAGTG
<i>Cebpb</i>	CAAGCTGAGCGACGAGTACA	TCAGCTCCAGCACCTTGTG
<i>Pou5f1</i>	AGAACCGTGTGAGGTGGAGT	CAAGCTGATTGGCGATGTGAG
<i>Nanog</i>	AAGGATGAAGTGCAAGCGGT	ATGCGTTCACCAGATAGCCC
<i>Rest</i>	CCGCTCAGATTGAGGTTGCT	CTTTTGGTTGGCTTACCCG
<i>Klf4</i>	CTTGACAGAGTAACAACCCG	CCGATTCTGTTGGGTTAGC
<i>Sox2</i>	TTTGTCCGAGACCGAGAAGC	CTCCGGGAAGCGTGTACTTA
<i>Myc</i>	TCCATCCTATGTTGCGGTCG	TGAAGGTCTCGTCGTCAGGA
<i>beta-actin</i>	AAATCGTGCGTGACATCAAAGA	GCCATCTCTGCTCGAAGTC
<i>18S</i>	TCGAACGTCTGCCCTATCAAC	TGGATGTGGTAGCCGTTTCTC
<i>Col1a2</i>	GAAATGGCAACTCAGCTCGC	TCCAGGTACGCAATGCTGTT
<i>Col5a1</i>	AAACCCAGGTTCTGGTTTCCAG	GGTCATTTGTACCACGCCCA
<i>Col5a2</i>	GAGTTTACGGAAGACCAGGCA	AATCATCACAAGTGCGGGCT
<i>Col5a3</i>	CGTGACGCCCTCAAGGTTTT	GAGGCCAGTTTACCCTCTC
<i>Col6a1</i>	GGGCGGCTCTTCAAGTTCTT	GCTTCCCGGTAGAAACGAGT
<i>Col6a2</i>	CAAGGGCAACATGGGTGAAC	TCCGACCATCCGATCCAAAT
<i>Col6a3</i>	CTGGAGAACGTGGCAGAACT	TTCACTGCCAACCCCATCTC
<i>Col15a1</i>	CTCAGCGACATGGGTGACAT	CCAACCATCTCGGACACGAA
<i>Col18a1</i>	GAGCCATGGGTGCCTCTG	ACAAAGATGAGCCAGCCCTC

**Table S2. Enriched genes of cell cluster and gene ontology analysis**

Cluster	Gene Ontology analysis	Top Enriched genes
0	Response to wounding, inflammation response, immune response, defense response, cellular homeostasis, cytokine-mediated signaling pathway, regulation of cell growth	Cxcl2, Gm12840, Ptx3, Cxcl1, Sbsn, Ccl2, Procr, Dmkn, Gfpt2, Has1, Eif4e, Ugdh, Ptgs2, Il6, Uap1, Mt2, Ngf, Igfbp4, Ier3, Rnd1
1	Extracellular matrix organization, response to oxidative stress, cell adhesion, biological adhesion, collagen fibril organization, vasculature development	Cxcl12, Igfbp3, Ctsk, Pltp, Postn, Mfap2, Gpx3, Serpinh1, Col1a1, Pcolce, Tgfb1, Txnip, Col3a1, Rcn3, Lgals1, Lpl, Aspn, Sfrp1, Aebp1, Lum
2	Response to protein stimulus, regulation of mRNA metabolic process, ossification, positive regulation of transcription, positive regulation of gene expression, regulation of cell cycle	Fos, Jun, Hspa1a, Myoc, Egr1, Gadd45g, Gas6, Gpx3, Dusp1, Cilp, Phlda1, Cyr61, Jund, Zfp36, Atf3, Cygb, Apod, Hspa8, Igf1, Mn1
3	Cell adhesion, biological adhesion, positive regulation of cell-substrate adhesion, regulation of cell-substrate adhesion	Thbs4, Cilp, Mgp, Smoc2, Fbln7, Bgn, Col8a1, Crlf1, Col6a2, Cxcl14, Lum, Col6a3, Mfap4, Fbln2, Hmcn2, Hsd11b1, Angpt1, Cd9, Col15a1, Serpinh1
4	Inflammation response, response to wounding, defense response, nitro oxide mediated signal transduction, blood vessel development, response to inorganic substance, response to metal ion	Cd44, Icam1, Emp1, Col1a2, Mt1, Col1a1, Lgals3, Tnfrsf12a, Ndrgr1, Mt2, Sdc4, Btg1, Gpha2, Ccl7, Col3a1, Serpina3n, Lmna, Ndufa4l2, Sphk1, Ccl19
5	Proteoglycan metabolic process, triglyceride metabolic process, acylglycerol metabolic process, neutral lipid metabolic process, glycerol ether metabolic process, organic ether metabolic process	Igfbp7, Cxcl14, Cst3, Lum, Cd9, Ecm1, Serpinh1, Cxcl12, Gas6, Tsc22d3, Cygb, Igf1, Steap4, Lpl, Fam150b, Gdf10, Cav1, Mgst3, Bgn, Fxyd5
6	Inflammatory response, response to wounding, defense response, immune response, nitric oxide mediated signal transduction, taxis, Chemotaxis, zinc ion homeostasis, cellular cation homeostasis	Mt2, Ccl2, Mt1, Cxcl1, Gm12840, Ccl7, Ugdh, Ptx3, Gfpt2, Igfbp4, Ptgs2, Zfp3611, Cxcl2, Metrnl, Kdm6b, Pim1, Pdpn, Dmkn, Nfkb1a, Tnfaip2
7	Response to wounding, inflammatory response, response to protein stimulus, regulation of cell proliferation, regulation of RNA metabolic process, negative regulation of myeloid cell differentiation	Anxa3, Sfrp2, Igfbp4, Plpp3, Pi16, Plac8, Pla1a, Il1r2, Efh1, Id3, Anxa1, Nr4a1, Dpp4, Ecm1, Cxcl13, Irf1, Efemp1, Prss23, Stmn4, Errf1
8	Negative regulation of signal transduction and cell communication, gland development, blood vessel morphogenesis, homeostatic process, negative regulation of protein kinase cascade, sterol homeostasis, cholesterol homeostasis	Cryab, Cfh, Mgst3, Igf1, Nme1, Spry2, Gm42418, Ctgf, Col15a1, Cav1, Apoe, Gdf10, Cbx3, Sh3bgrl3, Ccl8, Emp1, Inmt, Nrep, Slc39a1, Fosb
9	Extracellular matrix organization, skeletal system development, collagen biosynthetic process, collagen metabolic process, skin development, multicellular organismal metabolic process	Col1a1, Col1a2, Sparc, Col3a1, Cpz, Ndufa4l2, Ctsk, Cldn10, Aebp1, Kazald1, Ctsh, Pdgfrl, Rcn3, Mfap2, Cgref1, Tgfb1, Ctl2a, Sh3pxd2a, C1qtnf6, Serpinh1
10	Gland development, skeletal muscle tissue development, gland morphogenesis, extracellular structure organization, regulation of nitric oxide biosynthetic process, protein folding	Nme1, Timp1, Ran, S100a6, Isg15, Tnc, Hspe1, Anxa2, Vim, Tspo, Steap1, Emp1, Iigp1, Ddah1, Mndal, Zbp1, Cav1, Bst2, Slc25a5, Ddx39
11	Cell adhesion, cytoskeleton organization, cell-cell adhesion, cellular component organization, regulation of signal transduction, cell junction assembly, cell motion	Chodl, Igfbp2, Rarres1, Vim, Rasgrp2, Lmna, Lgals1, Wif1, Trps1, Aqp1, Robo2, Tagln, Lrrc15, Cd9, Fam180a, Lgals3, Csrp1, Bgn, Ramp1, Arhgdib
12	Blood vessel morphogenesis, blood vessel development, vasculature development, cell differentiation	Zc3h12a, Cxcl2, Nfkb1, Zfp3611, Ngf, Sbsn, Nr4a3, Hbb-bs
13	Cell cycle phase, cell cycle process, mitosis, nuclear division, cytoskeleton organization	Shc1, Nuf2, Ska1, BC030867, Cep55, Cdca5, Ccnb1, Ncapg, Mki67, Dlgap5, Esco2, Mis18bp1, Cdca3, Hmnr, Tpx2, Cenpf, Ndc80, Cdk1, Kif20a, Hist1h2ae
14	Chemotaxis, defense response, inflammatory response, response to wounding, immune response	Ccl4, C5ar1, Ms4a6c, Clec4a3, Cybb, Cd163, Fcrls, BC018473, Lill4b, C3ar1, Fcgr4, Msr1, Tlr7, Lyve1, Mrc1, Pld4, Ms4a6d, Mgl2, Fcna, Ccl12

Top enriched genes for each cluster, and gene ontology analysis of enriched genes in each cluster (David 6.7 version).

**Table S3. Cell cycle analysis of cells in different clusters**

Cluster	Total		G1		S		G2M		Undecided		% G1		% S		% G2M		% Undecided	
	GFP-	GFP+	GFP-	GFP+	GFP-	GFP+	GFP-	GFP+	GFP-	GFP+	GFP-	GFP+	GFP-	GFP+	GFP-	GFP+	GFP-	GFP+
0	1505	1947	993	1205	231	415	281	327	0	0	65.98	61.89	15.35	21.31	18.67	16.80	0.00	0.00
1	1019	1035	674	612	185	258	160	165	0	0	66.14	59.13	18.16	24.93	15.70	15.94	0.00	0.00
2	946	899	569	443	176	258	200	198	1	0	60.15	49.28	18.60	28.70	21.14	22.02	0.11	0.00
3	621	449	391	278	113	112	116	59	1	0	62.96	61.92	18.20	24.94	18.68	13.14	0.16	0.00
4	515	544	377	385	57	78	81	81	0	0	73.20	70.77	11.07	14.34	15.73	14.89	0.00	0.00
5	385	551	245	319	70	151	70	81	0	0	63.64	57.89	18.18	27.40	18.18	14.70	0.00	0.00
6	548	382	397	299	95	29	48	54	8	0	72.45	78.27	17.34	7.59	8.76	14.14	1.46	0.00
7	461	446	258	225	90	136	113	85	0	0	55.97	50.45	19.52	30.49	24.51	19.06	0.00	0.00
8	460	204	242	109	115	28	54	67	49	0	52.61	53.43	25.00	13.73	11.74	32.84	10.65	0.00
9	325	299	216	191	48	68	61	40	0	0	66.46	63.88	14.77	22.74	18.77	13.38	0.00	0.00
10	173	177	84	81	47	51	42	45	0	0	48.55	45.76	27.17	28.81	24.28	25.42	0.00	0.00
11	163	90	84	50	38	18	41	22	0	0	51.53	55.56	23.31	20.00	25.15	24.44	0.00	0.00
12	90	150	54	76	22	43	14	31	0	0	60.00	50.67	24.44	28.67	15.56	20.67	0.00	0.00
13	29	36	0	0	6	4	23	32	0	0	0.00	0.00	20.69	11.11	79.31	88.89	0.00	0.00
14	7	2	7	2	0	0	0	0	0	0	100.00	100.00	0.00	0.00	0.00	0.00	0.00	0.00
Total	7247	7211	4591	4275	1293	1649	1304	1287	59	0								

Left: The number of GFP- or GFP+ cells in different cell cycle stages of each cluster. Right: The ratio of GFP- or GFP+ cells in different cell cycle stages in each cluster (Seurat version 3).

**Figure S1**

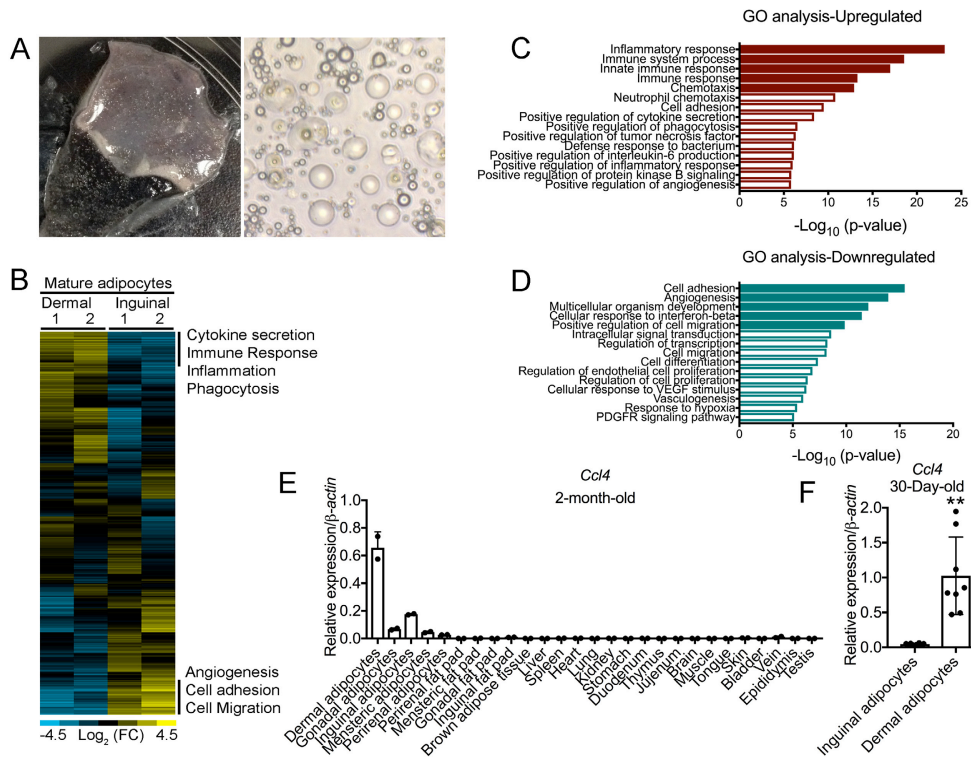


**Figure S2**

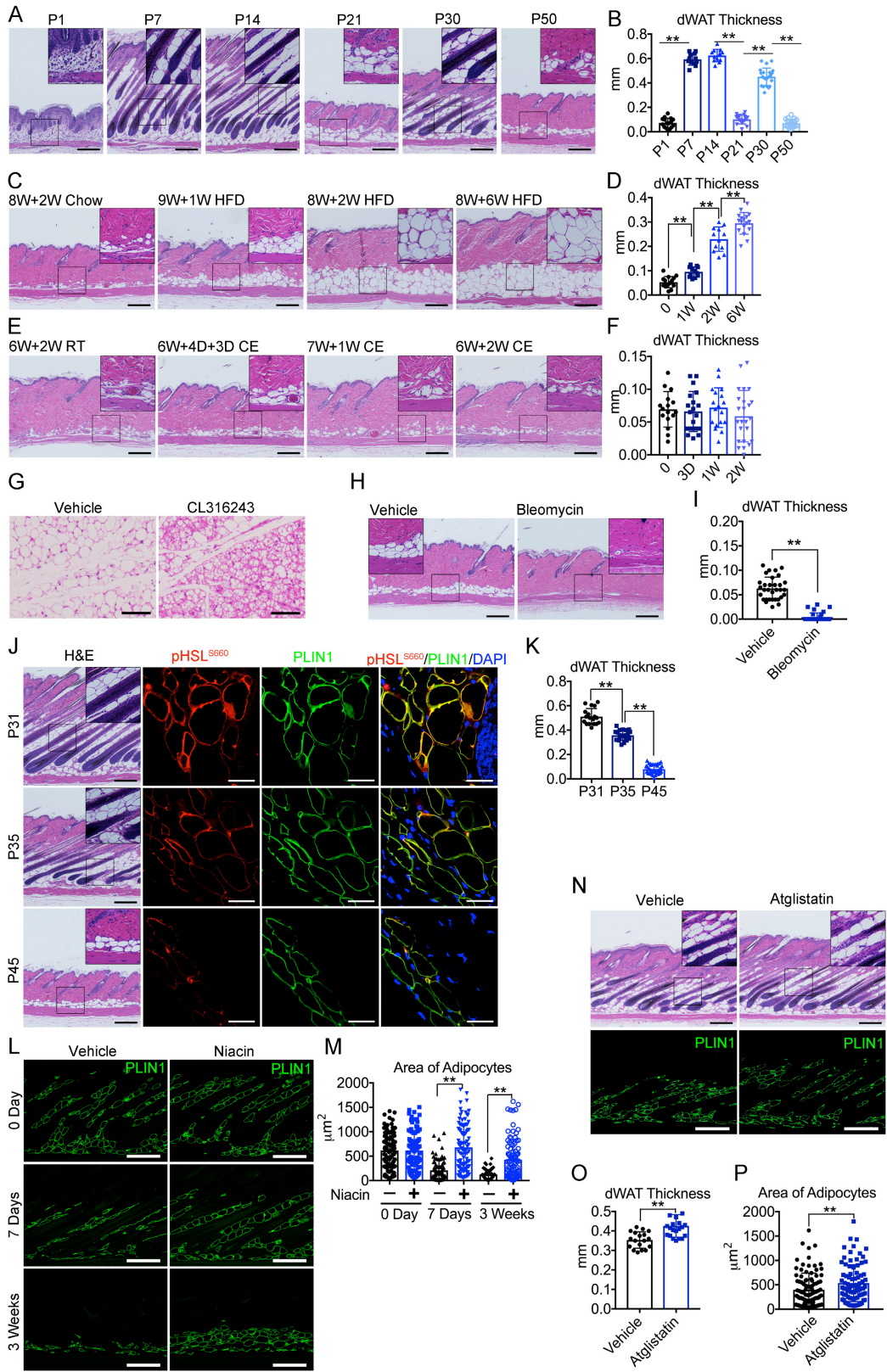


**Figure S3**

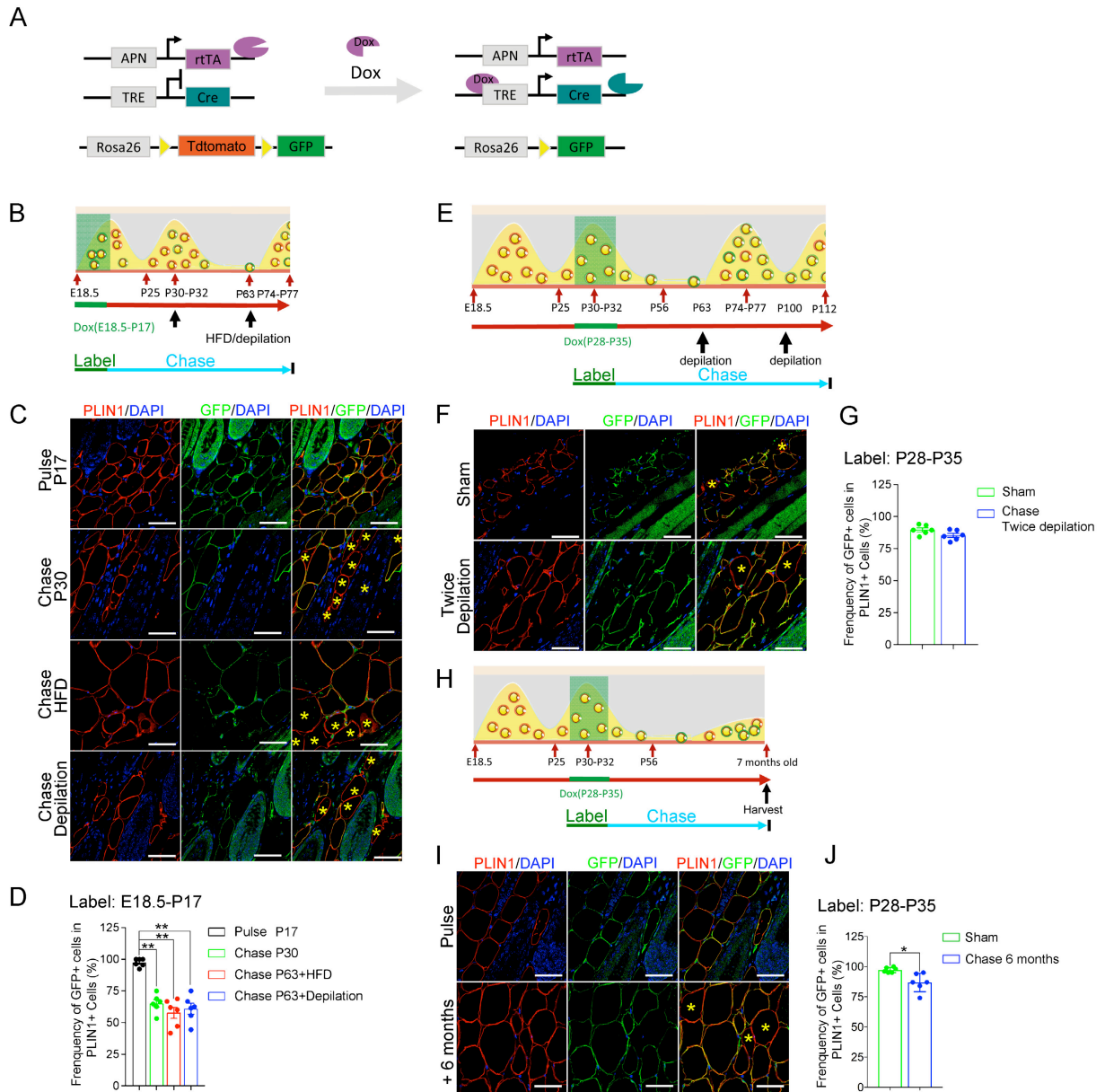
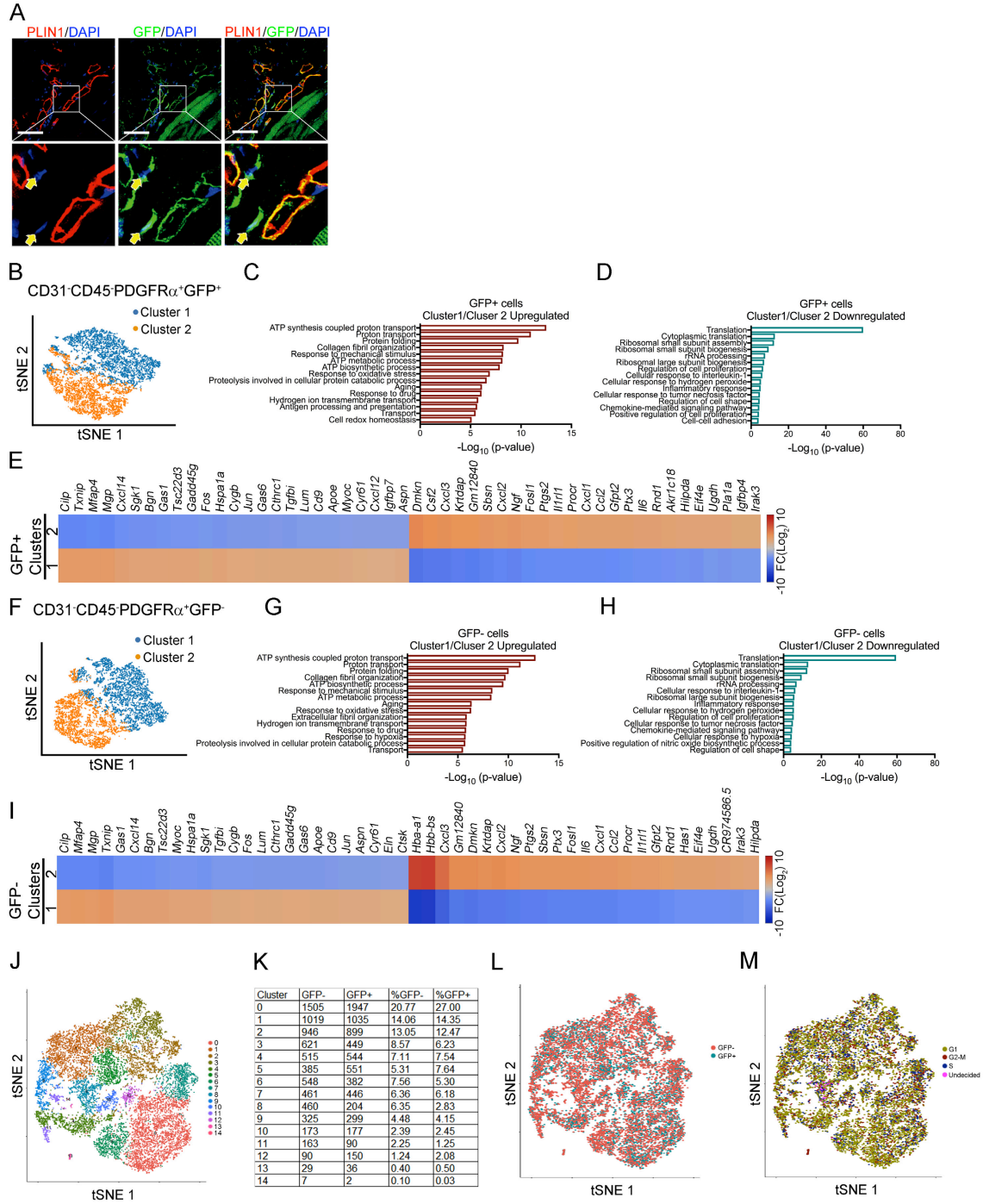
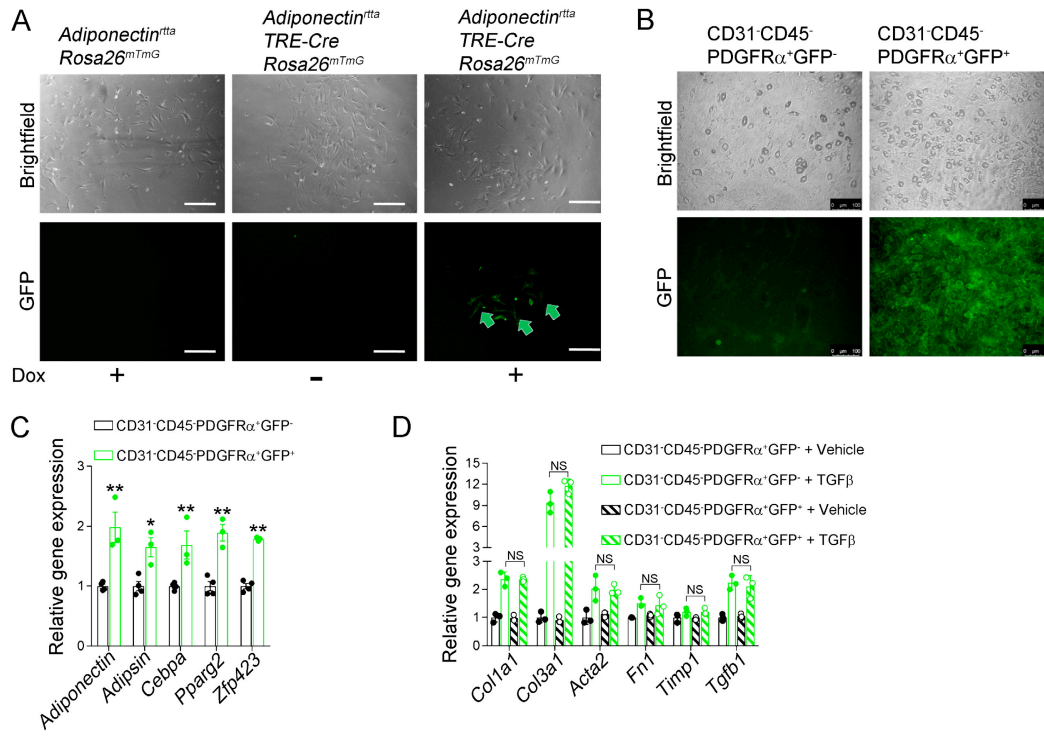


Figure S4



**Figure S5**



**Figure S6**

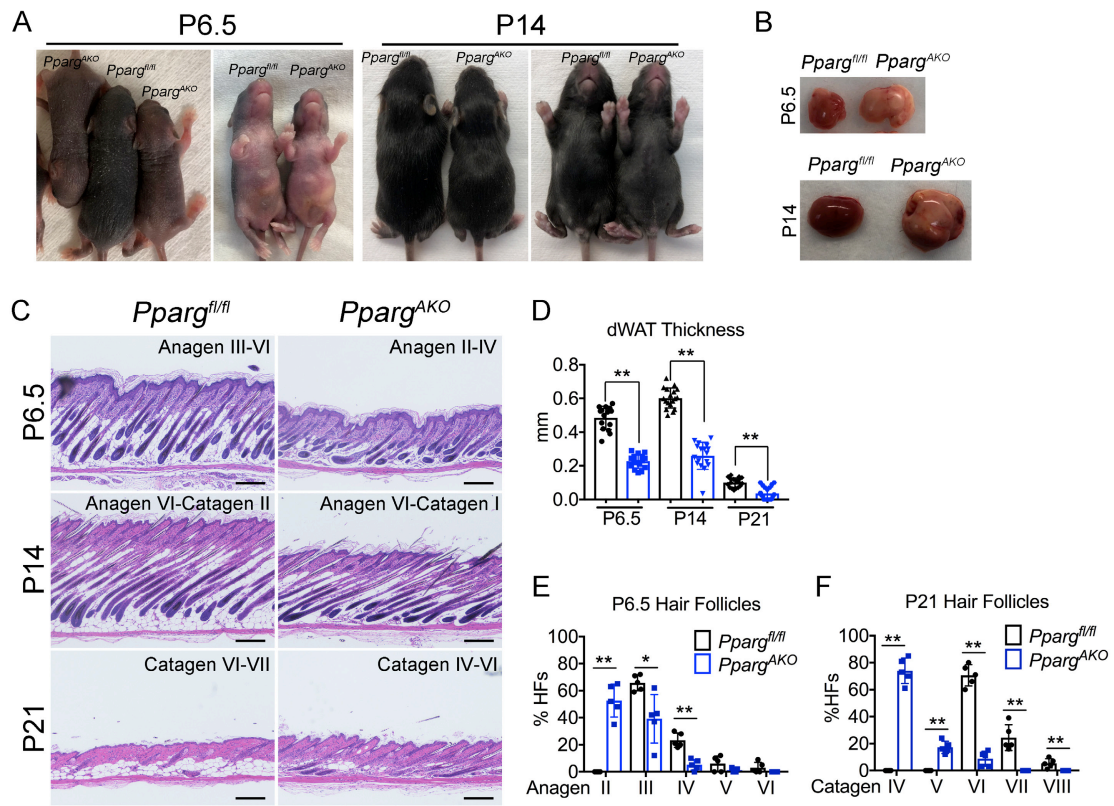


**Figure S7**

